Transactions of the Materials Research Society of Japan 29[7] 3005-3008 (2004)

Transformation behavior of Ti-Ni-Pt high temperature shape memory alloys

Yohei Takahashi[+], Tomonari Inamura, Junpei Sakurai,
Hideki Hosoda[++], Kenji Wakashima and Shuichi Miyazaki[*]

Precision and Intelligent Laboratory (*P&I Lab*), Tokyo Institute of Technology (*Tokyo Tech*)
4259 Nagatsuta, Midori-ku, Yokohama 226-8503, Japan
Phone&Fax: 81-45-924-5057, Email: hosoda@pi.titech.ac.jp ([++]corresponding author)
*Institute of Materials Science, University of Tsukuba, Tennodai 1-1-1, Tsukuba, Ibaraki 305-8573, Japan
Phone&Fax: 81-298-53-5283, Email: miyazaki@ims.tsukuba.ac.jp
[+]Graduate Students, Tokyo Institute of Technology
Phone&Fax: 81-45-924-5061, Email: yohei_t748@ken.pi.titech.ac.jp

Abstract : The martensitic transformation, the phase constitution and shape memory characteristics of Ti-Ni-Pt high temperature shape memory alloys (HTSMAs) were investigated by using X-ray diffraction analysis (XRD) from 100K to 600K, transmission electron microscopy (TEM), differential scanning calorimetry (DSC) from 300K to 800K and tensile tests at room temperature. Ti-Ni-Pt HTSMAs used were Ti-35Ni-15Pt and Ti-30Ni-20Pt. It was found by XRD and TEM that the martensite phase of both Ti-35Ni-15Pt and Ti-30Ni-20Pt is B19 in the temperature region investigated in this study. The martensitic transformation temperature M_s of Ti-35Ni-15Pt and Ti-30Ni-20Pt alloys are 453K and 517K, respectively, by DSC. By the tensile tests the ultimate tensile strength and the elongation of Ti-35Ni-15Pt were 280MPa and 6%, respectively. The alloy deformed at RT showed perfect shape recovery when deformed up to 4% and then heated above 473K ($>A_f$). Ti-35Ni-15Pt HTSMA exhibits a good combination of high transformation temperature, good shape memory properties and moderate mechanical properties. Therefore, the Ti-Ni-Pt alloys are hopeful for the high temperature applications which require actuation above the boiling temperature.

Key words: TiNi, Pt, high temperature shape memory alloy, martensitic transformation, shape recovery

1. INTRODUCTION

Ti-Ni shape memory alloy (SMA) is a representative smart material due to the unique characters of shape memory effect (SME) and superelasticity (SE). A limitation of the Ti-Ni SMA for practical applications is that the highest actuation temperature is around 400K for the binary Ti-Ni [1]. Thus, high-temperature shape memory alloys (HTSMAs) exhibiting higher actuation temperatures and comparable mechanical properties are eagerly required in the filed of automotives, aircrafts and engines, for example [2]. Large efforts have been paid in order to change the martensitic transformation temperature (M_s) of Ti-Ni by adding substitutional elements. It is known that most ternary elements such as Fe, Co and Cr reduce M_s of Ti-Ni [3-4] but that some substitutional elements such as Zr, Hf, Pd and Pt raise M_s [5-8]. Especially, Pt addition dramatically raises M_s and M_s of TiPt reaches around 1300K [6-10]. Based on the background, our group has made a systematic work for Ti-Ni base HTSMAs in terms of platinum-group metals (PGMs) [11-16]: the PGMs have a tendency to increase M_s due to their large atomic sizes and to substitute for the Ni-sites of TiNi [12]. Especially, it was found that M_s of TiNi-TiPt pseudobinary alloys proportionally increases up to 1300K with increasing Pt concentration when Pt content is more than 10mol% and that the Ti-Ni-Pt alloys containing 10-30mol%Pt exhibit moderate mechanical properties [12, 15]. It was also revealed that the apparent martensite phase is B19' monoclinic phase when Pt content is less than 10mol% and B19 orthorhombic phase when more than 20mol%[15]. Then, Ti-Ni-Pt alloys having 15 and 20mol%Pt were focused in this paper, and the phase transformation behavior was investigated in detail.

2. EXPERIMENTAL PROCEDURE

Two kinds of Ti-Ni-Pt pseudobinary alloys containing 50mol%Ti (the stoichiometric compositions) were used and the concentrations of Pt selected were15mol% and 20mol%. Hereafter, the alloys are called Ti-35Ni-15Pt for 50mol%Ti-35mol%Ni-15mol%Pt and Ti-30Ni-20Pt for 50mol%Ti-30mol%Ni-20mol%Pt. Starting materials were high purity elements of 99.99%Ti, 99.99%Ni and 99.9%Pt, and button ingots of both Ti-35Ni-15Pt and Ti-30Ni-20Pt were made by arc-melting method in Ar-1%H_2 with a non-consumable W electrode. The weight of button ingots was 5g for each, approximately. No chemical analysis was made for the alloys because the weight changes during processing were less than 0.1wt%. After alloying, the

ingots were hot-forged into disks with the thickness less than 1mm at 1473K for 10.8ks in an Ar atmosphere. The test specimens were cut from the disks by electro-discharge machining and polishing mechanically. Then, they were solution-treated at 1173K for 1.8ks by a ULVAC infrared image furnace in vacuum and supplied for the measurements.

The constituent phases were identified by conventional θ-2θ XRD analysis with CuKα using a Philips X'pert PRO system with X'celerator. The measurements were done in a temperature range from 100K to 600K in vacuum using a heating-cooling stage. In XRD measurements the specimens were firstly cooled down to 100K and then heated up to 600K. Transmission electron microscopy observation was carried out as supplements for the phase identification using Philips CM200 operated at 200kV. Thin foils for TEM observations were made by Ar ion-milling.

The phase transformation temperatures were measured by DSC using Shimadzu DSC-60 and Netzsch STA449C Jupiter in a temperature range from 300K to 800K with a heating/cooling rate of 10K/min. Tensile tests were conducted at RT using a Shimadzu Autograph Instron-type machine at the strain rate of 1.0×10^{-3}/s. The gauge size of tensile specimens for tensile tests is 2mmx0.2mmx20mm. In order to clarify the shape memory properties, some specimens were deformed to 4% in strain and heated over the reverse martensitic transformation finish temperatures (A_f).

3. RESULTS AND DISCUSSION

3.1 Phase constitution

Binary TiNi and TiPt undergo martensitic transformations to monoclinic B19' and orthorhombic B19, respectively [5, 6]. In our previous work it was found by XRD at RT that B2 and/or B19' (monoclinic) phases appear when Ti-Ni-Pt contains less than 10mol%Pt whilst B19 (orthorhombic) phase when Ti-Ni-Pt contains more than 20mol%Pt. Therefore, it has been deduced that the critical Pt concentration above which B19 is the stable crystal structure of the martensite is located between 10~20mol%Pt [4].

Figure 1 shows XRD profiles at various temperatures during heating from 100K to 600K for (a) Ti-35Ni-15Pt and (b) Ti-30Ni-20Pt. It was seen in Fig. 1 (a) that B19 orthorhombic phase (o) is the martensite phase for both Ti-35Ni-15Pt and Ti-30Ni-20Pt. The diffraction peaks indicated by 'x' were from the XRD instrument.

In Ti-35Ni-15Pt, it was seen that B19 and B2 coexist at temperatures between 300K and 600K. B2 parent phase began to appear between 300K and 400K during heating. Therefore, the reverse martensite transformation

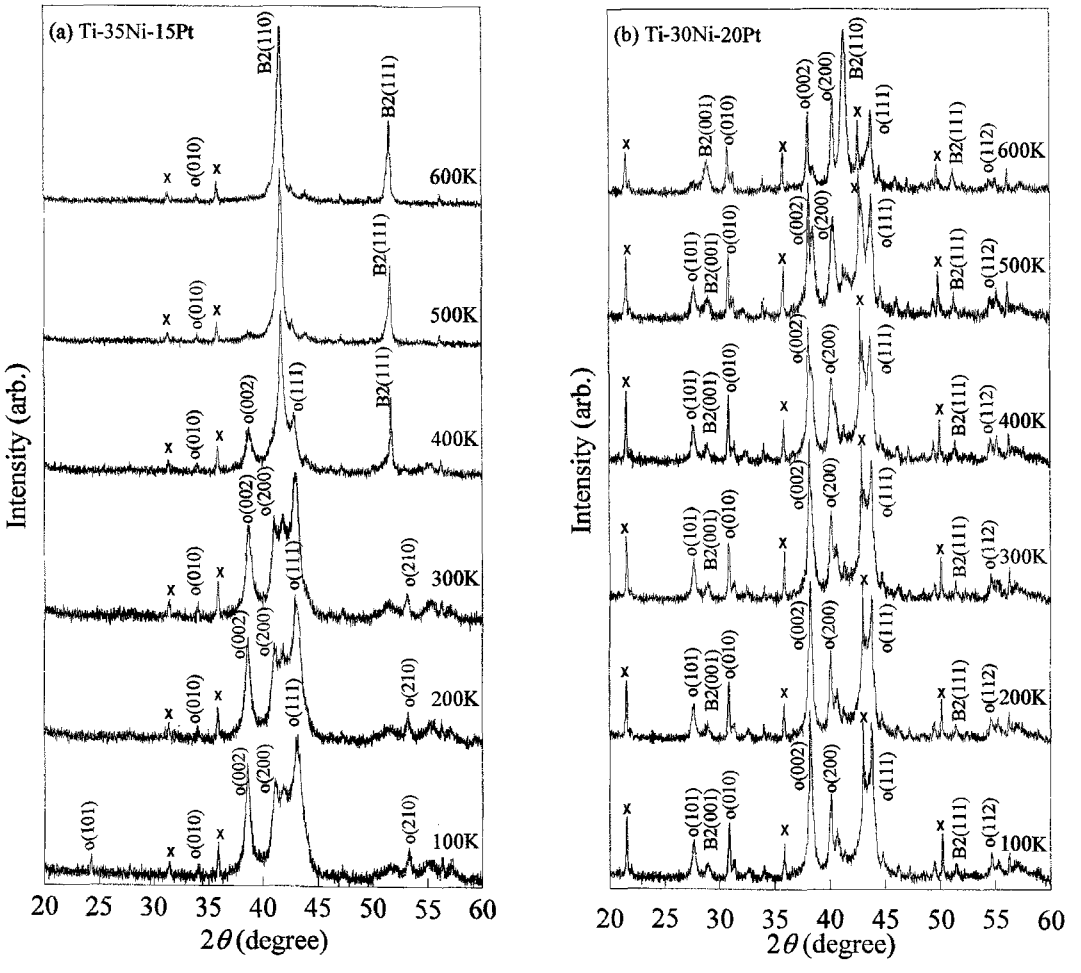

Figure 1 Selected XRD profiles obtained for (a) Ti-35Ni-15Pt and (b) Ti-30Ni-20Pt at temperatures from 100 to 600K. The letters "o" stands for the orthorhombic B19 structure, respectively.

start temperature (A_s) lies between these temperatures. Besides, the reflections from B19 still exist at 600K. The reverse martensite finish temperature (A_f) is judged to be higher than 600K as far as judging from XRD.

Ti-30Ni-20Pt was also composed of B19 at 100 K, and the B2 parent phase clearly appeared at 600K. The reflections from B2 seem to exist at 500K. However, the existence of B2 phase at 500K was not perfectly confirmed since the peak profiles of martensite phases are complicated and the peaks are weak near A_s. By comparing Fig. 1 (a) and (b), it is found that A_s is higher in Ti-30Ni-20Pt than in Ti-35Ni-15Pt due to the larger content of Pt.

TEM observation was also carried out in Ti-35Ni-15Pt alloy to confirm the crystal structure of martensite. Figure 2 shows electron diffraction patterns taken from a single variant of martensite in Ti-35Ni-15Pt. The specimen was systematically tilted around some low-indexed poles and the crystal structure was analyzed. It was confirmed that the electron diffraction patterns taken in Ti-35Ni-15Pt can not be indexed with monoclinic B19' but with orthorhombic B19, as demonstrated in Figure 2. No martensite with B19' structure was observed in this study.

According to the results of XRD measurement and TEM observation, the crystal structure of the martensite in Ti-35Ni-15Pt was determined to be B19. No significant evidence of B19→B19' transformation during cooling was obtained in the alloys with more than 15mol%Pt in the present crystal structure analysis.

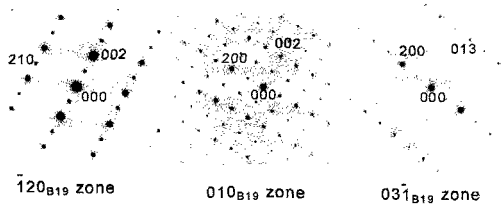

Figure 2 Indexed diffraction patterns of Ti-35Ni-15Pt

3.2 Phase transformation temperatures

Figure 3 shows DSC heating and cooling curves obtained for (a) Ti-35Ni-15Pt and (b) Ti-30Ni-20Pt. It is found for DSC cooling curve in Fig.3 (a) that martensitic transformation start temperature M_s and finish temperature M_f of Ti-35Ni-15Pt is 453K and 380K, respectively. A_s and A_f are 447K and 473K, respectively. A_s obtained by DSC is slightly different from that judged from XRD results. Besides, two-step-like phase transformation appears in the cooling curve but single peak is seen in the heating curve. The two-step-like peak may be due to two-step martensite transformation. However, no evidence of two-step transformation was confirmed in crystal structure analysis at present. This point requires further investigation.

On the other hand for Ti-30Ni-20Pt, M_s, M_f, A_s and A_f are judged to be 516K, 473K, 493K and 540K, respectively. A_s of 493K is close to that estimated from the XRD results. However, both DSC heating and cooling curves exhibit single peak, different from those of Ti-35Ni-15Pt.

3.3 Tensile and shape memory properties

Figure 4 (a) shows the tensile stress-strain curves of Ti-35Ni-15Pt and Ti-30Ni-20Pt at RT. The yield stress ($\sigma_{0.2}$), ultimate tensile strength (UTS) and fracture strain were 100MPa, 280MPa and 6% for Ti-35Ni-15Pt, respectively. Those for Ti-30Ni-20Pt were 400MPa, 620MPa and 6%, respectively. The fracture strain of both alloys is almost the same value regardless of the difference in yield stress and UTS. Since the yield stress of SMAs in general corresponds to reorientation of martensite variants when the test temperature is below M_s, the stress required for reorientation of martensite variants is much higher in Ti-30Ni-20Pt ($\sigma_{0.2}$: 400MPa) than that of Ti-35Ni-15Pt ($\sigma_{0.2}$: 100MPa). The difference in yield stress must also depend on microstructure, which is now being investigated by TEM.

Figure 4 (b) shows shape recovery by heating in Ti-35Ni-15Pt. It is clear that this alloy exhibits perfect shape recovery around 2.4% by heating. Besides, some pseudoelastic shape recovery about 0.5% was seen by unloading only. The pseudoelasticity must be due to small amount of dislocations introduced during deformation in the solution-treated alloy. By taking into account the high M_s above 450K, this alloy is a candidate as a practical HTSMA.

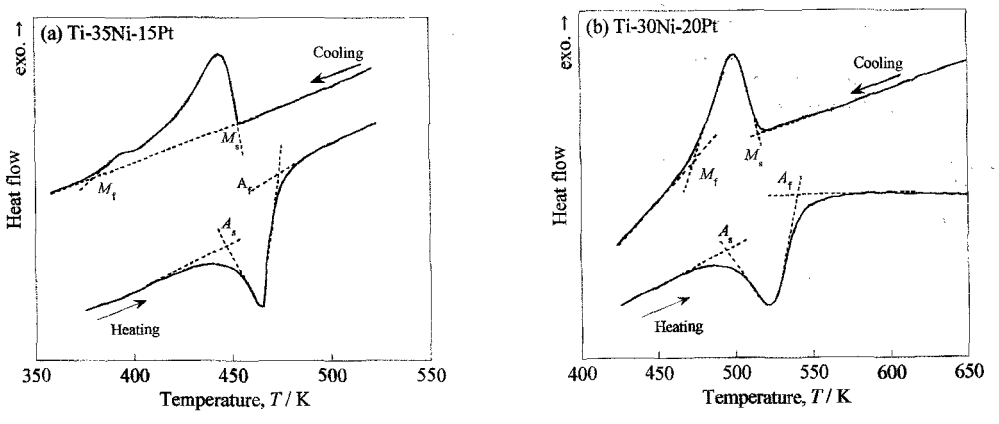

Figure 3 DSC heating and cooling curves of (a) Ti-35Ni-15Pt and (b) Ti-30Ni-20Pt.

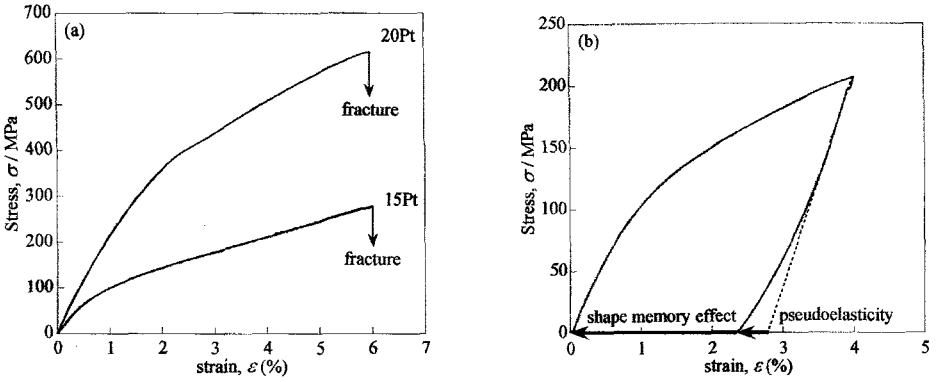

Figure 4 The tensile stress-strain curves of (a) Ti-35Ni-15Pt and Ti-30Ni-20Pt and (b) shape recovery of Ti-35Ni-15Pt by heating after unloading from 4% strain. It is noted that the perfect shape recovery was seen for (b).

4. Conclusions

(1) Ti-35Ni-15Pt and Ti-30Ni-20Pt have B19 orthorhombic phases as martensite phases.

(2) Judging from XRD results A_s of Ti-35Ni-15Pt and Ti-30Ni-20Pt are between 300k and 400K and near 500K, respectively.

(3) M_s, M_f, A_s and A_f of Ti-35Ni-15Pt obtained by DSC are 453K, 383K, 447K and 473K, respectively. And also M_s, M_f, A_s and A_f of Ti-30Ni-20Pt obtained by DSC are 516K, 473K, 493K and 540K, respectively.

(4) A_s obtained by DSC is slightly different from that estimated by XRD. Two-step-like phase transformation appears in the cooling curve of Ti-35Ni-15Pt.

(5) The yield stress, ultimate tensile strength and fracture strain are 100MPa, 280MPa and 6% for Ti-35Ni-15Pt, respectively. Those for Ti-30Ni-20Pt are 400MPa, 620MPa and 6%, respectively.

(6) Ti-35Ni-15Pt exhibits perfect shape recovery by heating after deformation up to 4%.

(7) Since Ti-35Ni-15Pt exhibits good shape memory effect and moderate mechanical properties, Ti-35Ni-15Pt is a candidate as a practical HTSMA applied for above the boiling temperature.

5. Acknowledgements

This work was partially supported by Grant-in-Aid for Fundamental Scientific Research (Wakate A: No.14703016) and the 21st COE Program from the Ministry of Education, Culture, Sports, Science and Technology, Japan, and Osawa Science Studies Grants Foundations.

6. References

[1] T. Saburi, "Ti-Ni shape memory alloys", *Shape Memory Alloys*, eds. K. Ohtsuka and C. M. Wayman, Cambridge University Press, (1998) pp.49-96.

[2] D. Goldberg, Ya Xu, Y. Murakami, S. Morito, K. Otsuka, T. Ueki and H. Horikawa, *Intermetallics*, **3** (1995) 35.

[3] K. H. Eckelmeyers, *Scr. Metall.*, **10** (1976) 667.

[4] T. Honma, M. Matsumoto, Y. Shugo, M. Nishida and I. Yamazaki, *TITANIUM'80 Science and Technology*, ed. by O. Izumi, **2** (1980) 1455.

[5] J. V. Humbeek and G. Firstov, *The Fourth Pacific Rim Intl. Conf. On Advanced Materials Processing (PRICM-4)*, eds. S. Hanada, Z. Zhong, S. W. Nam and R. N. Wright, Jpn. Inst. Metals, **2** (2001) 1871.

[6] H. C. Donkersloot, and J. H. N. Van Vucht, Less-Common Mat., **20** (1970) 83-91.

[7] V. N. Khachin, N. A. Matveeva, V. P. Sivokha and D. V. Chernov, *Dokl. Acad. Nauk SSSR* **257**, 167 (1981).

[8] V. Kolomytsev, *Scripta Metall.*, **31**, 141 (1994).

[9] T. Biggs, M. J. Wicomb, and L.A. Cornish, *Materials Science & Engineering A*, **A273-275** (1999) 204-207.

[10] T. Biggs, M. B. Cortie, M. J. Wicomb, L.A. Cornish, *Metall. Mater. Trans. A*, **32A** (2001) 1883.

[11] H. Hosoda, M. Tsuji, Y. Takahashi, T. Inamura, *2nd Intl. Conf. on Advanced Fiber/Textile Materials 2002 in Ueda with Forum of Asian Young Scientists on Fiber/Textile Materials*, (2002) 95.

[12] H. Hosoda, M. Tsuji, M. Mimura, Y. Takahashi, K. Wakashima and Y. Yamabe-Mitarai, *Defect Properties and Related Phenomena in Intermetallic Alloys*, eds. E. P. George, H. Inui, M. J. Mills, G. Eggeler, Mat. Res. Soc. Symp. Proc., **753** (2003) BB5.51.

[13] M. Tsuji, H. Hosoda, K. Wakashima and Y. Yamabe-Mitarai, *ibid*, BB5.52.

[14] H. Hosoda, M. Tsuji, Y. Takahashi, T. Inamura, K. Wakashima, Y. Yamabe-Mitarai, S. Miyazaki and K. Inoue, *Materials Science Forum*, **426-432** (2003) 2333.

[15] Y. Takahashi, M. Tsuji, J. Sakurai, H. Hosoda, K. Wakashima, S. Miyazaki, *MRS-J*, **28** (2003) 627-630.

[16] H. Hosoda, Y. Takahashi, Y. Fukui, T. Inamura, K. Wakashima and S. Miyazaki, *First Intl. Congress on Bio-Nanointerface (ICBN2003)*, (2003) 191.

(Received October 10, 2003; Accepted March 20, 2004)